IEEE Access
Multidisciplinary | Rapid Review | Open Access Journal

Received August 10, 2019, accepted August 25, 2019, date of publication September 11, 2019,
date of current version September 24, 2019.

Digital Object Identifier 10.1109/ACCESS.2019.2940273

Independent Matching Dual-Band Compact Quarter-Wave Half-Slot Antenna for Millimeter-Wave Applications

MOHAMED ABOUALALAA[1,2,3], (Member, IEEE), ISLAM MANSOUR[4], HALA ELSADEK[1], (Senior Member, IEEE), ADEL B. ABDEL-RAHMAN[2,5], AHMED ALLAM[2], MOHAMMED ABO-ZAHHAD[2,6], (Senior Member, IEEE), KUNIAKI YOSHITOMI[3], (Member, IEEE), AND RAMESH K. POKHAREL[3], (Member, IEEE)

[1]Microstrip Department, Electronics Research Institute, Giza 12622, Egypt
[2]School of Electronics, Communications and Computer Engineering, Egypt-Japan University of Science and Technology (E-JUST), New Borg El Arab City, Alexandria 21934, Egypt
[3]Faculty of Information Science and Electrical Engineering, Kyushu University, Fukuoka 819-0395, Japan
[4]Electrical Engineering Department, Faculty of Engineering, Shoubra, Benha University, Cairo 11629, Egypt
[5]Electrical Engineering Department, Faculty of Engineering, South Valley University, Qena 83523, Egypt
[6]Electrical Engineering Department, Faculty of Engineering, Assiut University, Assiut 71515, Egypt

Corresponding author: Mohamed Aboualalaa (mohamed.ali@ejust.edu.eg)

This work was supported in part by the Grant-in-Aid for Scientific Research (C) under Grant JP 16K06301, in part by the VLSI Design and Education Center (VDEC), and in part by the University of Tokyo in collaboration with Cadence and Keysight Corporations.

ABSTRACT A dual-band mm-wave compact antenna is proposed in this paper. A quarter-wave half-slot resonator is used instead of a half-wave slot to achieve miniaturization of the antenna size. The antenna consists of two stacked half-slot resonators to radiate at two frequencies, $f_1 = 24\ GHz$ and $f_2 = 28.5\ GHz$, with the same microstrip line feed. By using this stacked structure, a dual-band is obtained and the two resonant frequencies become independently matched with a minor effect on each other. Measurements show the proposed antenna has an impedance bandwidths of 6.3% and 15% at f_1 and f_2, respectively; furthermore, the antenna has good radiation characteristics. The antenna gains in addition to the radiation efficiencies at f_1 and f_2, are $3.5dBi$, 92%, $4dBi$, and 95% respectively. The equivalent circuit model for the proposed antenna is introduced to show the electrical behavior of the antenna. Finally, the antenna design is inserted in multiple-input multiple-output (MIMO) system. The proposed antenna is analyzed and optimized using ANSYS HFSS EM simulator and its equivalent circuit is performed by Agilent Advanced Design System (ADS). The simulated as well as measured results show good agreement. The designated antenna resembles good candidate for 5G wireless communication systems.

INDEX TERMS Compact antenna, dual frequency, independent matching, multiple-input multiple-output (MIMO), quarter-wave half-slot resonator (QWHSR), stacked structure.

I. INTRODUCTION

The existing mobile communication spectrum at low frequency bands is facing many problems concerning the communication speed like having low bit rate and cannot keep up with the tremendous development in the communication sector in the near future. Therefore, many research works tended to study the feasibility of using 5G wireless communication [1]–[7]. Consequently, many antenna designs are introduced at 5G mm-waves [8]–[12]. In [8], a 5G broadband printed dipole antenna is presented. The single element antenna, with $10 \times 4.5\ mm^2$ antenna size, radiates from $26.5 - 38.2\ GHz$ with average gain around $5\ dBi$. A wide band high gain antenna array was introduced [9], four elements antenna array which works over a band from 23 GHz to 32 GHz with an antenna array gain between $10 - 12\ dBi$ for $5.35 \times 21.4\ mm^2$ array size. A single element is also introduced to get a gain of $5.3\ dBi$ at center frequency of $31.5\ GHz$ with $5 \times 5\ mm^2$ antenna size [10]. In [11], a single band vertically stacked folded dipole antenna for mm-wave applications is introduced. The antenna's dimensions are $5 \times 5\ mm^2$ which is designed at $28\ GHz$ with a peak gain of $5.67\ dBi$. Reflectarrays with high gain and high efficiency for 5G communications are summarized in [12]. In [13], eight elements Vivaldi antenna

The associate editor coordinating the review of this manuscript and approving it for publication was Sandra Costanzo.

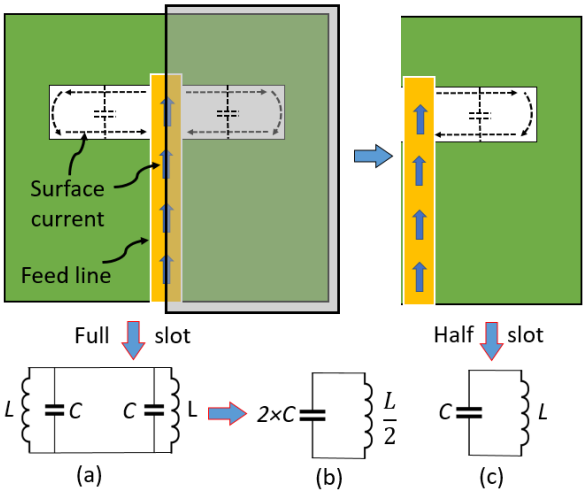

FIGURE 1. Equivalent model of full and half slots.

array with dimensions of $28.82 \times 60\ mm^2$ is introduced to work with 5G mmwave applications. Also a single band tilted combined beam antenna for $28GHz$ band was presented [14].

There are several studies for applying 5G antennas in MIMO systems [15]–[18]. A broadband circularly polarized (CP) Fabry–Perot resonant antenna for the fifth-generation (5G) wireless multipleinput-multiple-output (MIMO) is proposed in [15]. Coupling reduction is introduced in [16], [17] for 5G millimeter wave MIMO dielectric resonator antennas. In [18], a different configurations of 2×2 MIMO antenna arrays where eight types of antenna arrays are discussed with different polarizations.

In this work, a compact dual-band QWHSR antenna is designed which is an extension of a previous single band half-slot antenna [19]. Starting from the conventional half-wave slot antenna, where it is an inverse case of the strip patch antenna; therefore, there is a magnetic wall at the center of the slot, so the equivalent model for this full slot resonator can be represented by two parallel LC resonance circuits as shown in Fig. 1 (a). Hence, in case of the full slot antenna, the total equivalent inductance is equal $L/2$ while the total capacitance becomes $2 \times C$ as depicted in Fig. 1 (b). Consequently, by implementing QWHSR antenna which means the equivalent capacitance will be halved; On the other hand, the equivalent inductance will be doubled as illustrated in Fig. 1 (c). Therefore, the resonant frequency should be the same. In fact, the resonant frequency is slightly decreased owing to confining the field on only half slot resonator. In the presented paper, a QWHSR antenna is designed to achieve a small size with dual band operation at millimeter wave frequency range. The antenna has a stacked structure to achieve an independent matching dual band. At the last section of the paper, a study of 2×2 MIMO system using four elements of proposed antenna is introduced

II. ANTENNA GEOMETRY

The proposed stacked antenna comprises a common transmission line, with a width of $0.2mm$, which excites two ground

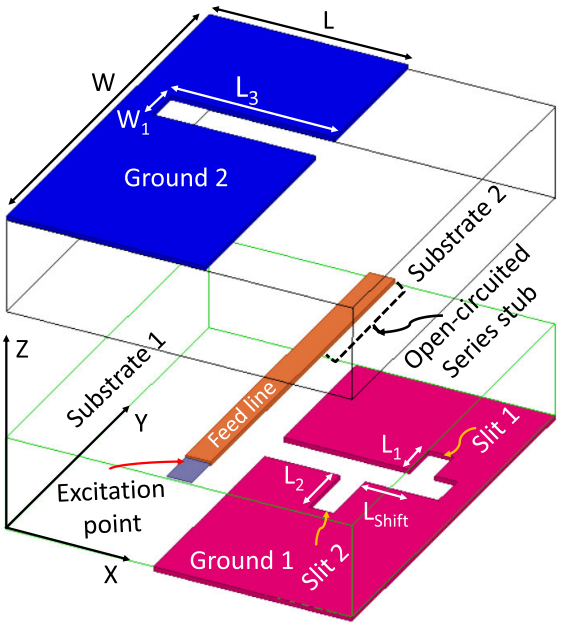

FIGURE 2. Antenna geometry; $L = 1.5mm$, $W = 3.2mm$, $W_1 = 0.3mm$, $L_1 = 0.3mm$, $L_2 = 0.5mm$, $L_3 = 1.3mm$, $L_{Shift} = 0.4mm$.

planes, the lower one contains a half slot with two slits inside as shown in Fig. 2; this half slot in addition to the two slits are designed to resonate at the lower frequency band. While, the upper ground plane has another rectangular half slot which is assigned for the higher frequency band. The two ground planes are connected from their edges. An open-circuited series stub shown in Fig. 2 is used for adjusting the antenna matching at the two frequency bands. The proposed antenna is designed on Rogers Duroid RO3003 with a relative permittivity (ϵ_r) of 3, substrate thickness (h) of 0.76 mm, a dielectric loss tangent ($tan\delta$) of 0.0013 and a copper thickness (t) of 0.017 mm. The antenna geometrical parameters are illustrated in Fig. 2.

Due to the small dimensions of the proposed antenna, $2.7\ mm \times 3.2mm$, hence the transmission line is extended by $\lambda_g/2$ to fix the K connector during the antenna measurements, where λ_g is the guided wavelength and this extension means moving one complete cycle on the Smith chart, so the antenna input impedance should be the same value. The proposed antenna has dual-band of operation, so in the measurement it is difficult to achieve the matching at the two bands simultaneously after adding a certain length for connector soldering. Therefore, a dual band matching circuit is required for the measurements. In order to overcome this issue, the measurement process was simplified by dividing it into two steps, the first step is by extending the feeding line by $\lambda_g/2$ at the first resonant frequency (f_1) where $\lambda_g/2|_{f_1} = L_{ext1} = 3.6mm$. Then, after measuring the antenna characteristics (S_{11} and radiation patterns), the transmission line is shortened to give the extended length at $\lambda_g/2$ of the second higher resonating frequency to complete the antenna measurements in this case, where $\lambda_g/2|_{f_2} = L_{ext2} = 3mm$. Fig. 3 shows a photo of both

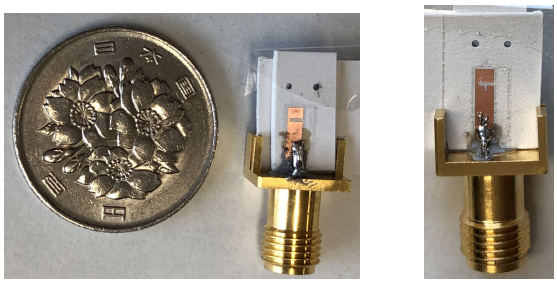

FIGURE 3. Photos of the fabricated antenna.

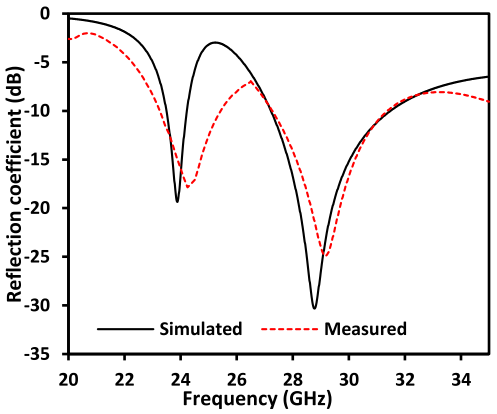

FIGURE 4. Simulated and measured $|S_{11}|$ results.

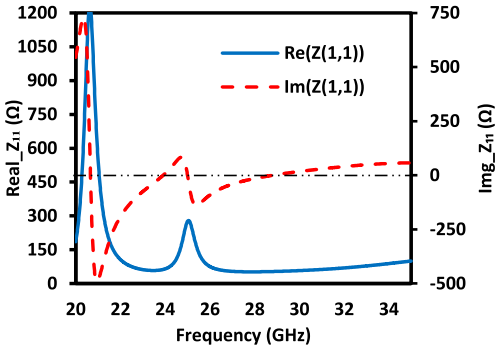

FIGURE 5. Input impedance of proposed antenna.

sides of the fabricated antenna prototype; the feeding line is confined between the two ground planes. The fabrication is accomplished by using CNC machine which gives an accurate dimensions at this high frequency range of operation.

III. RESULTS AND DISCUSSION

A. ANTENNA S-PARAMETERS

The simulated results using HFSS as well as the measured results of the antenna reflection coefficient for the proposed antenna at the two resonant frequencies are shown in Fig. 4. The first resonant frequency is $f_1 = 24\ GHz$ with the measured bandwidth of $1.53GHz$, while the higher resonant frequency is $f_2 = 28.5\ GHz$ with bandwidth of $4.5GHz$. The real and imaginary parts of the antenna input impedance are depicted in Fig. 5. For the sake of obtaining the optimal parameters affecting the performance characteristics of the proposed antenna in terms of impedance matching and operating bandwidth, the optimization of the key parameters are performed by ANSYS high-frequency structure simulator (HFSS). Figs. 6(a) and (b) show the effect of changing the slits' lengths of the half slot located on ground (1) (L_1 and L_2). The figures clear that by changing the lengths L_1 and L_2, this affects only on the first resonant frequency without significant impact on f_2. Similarly, L_3 only affects on the higher resonant frequency. Therefore, the two bands are controlled independently. Fig. 6(d) reveals the effect of changing the length of the upper half slot on the higher operating frequency (f_2), as evident from the figure, by increasing the upper half slot length, f_2 is decreased; L_3 is changing from $1mm$ to $2mm$, while its resonant frequency is varied from $25.5GHz$ to $32.5GHz$ without affecting on f_1. Another point to consider is that the length of slit (1), L_1, has more effect than L_2, this is because slit (1) is near to the half slot end where the confined field is concentrated as shown from the surface current distribution illustrated in Fig. 9(a). Also, the distance between the two slits, L_{Shift}, is studied, at the small values of L_{Shift} which means a large coupling between the two slits, then the first operating frequency decreases as depicted in Fig. 6(c). By choosing a suitable design parameters, the required dual-band frequencies as well as a wide bandwidth are obtained with minimum reflection coefficients at the two frequencies. The matching at the two bands can be adjusted by connecting a series stub with the feed line; Fig. 7 shows the effect of changing the stub length (L_{Stub}). To examine the effect of changing the substrate thickness on reflection coefficient $|S_{11}|$, a study of using a different thickness values are carried out as shown in Fig. 8. Substrate

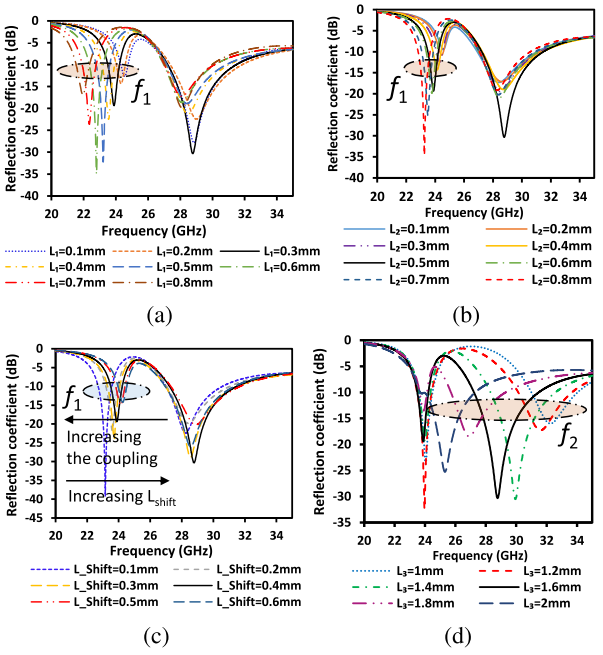

FIGURE 6. Parametric study for the different antenna parameters (a) effect of L_1 (b) L_2 (c) L_{Shift} (d) L_3.

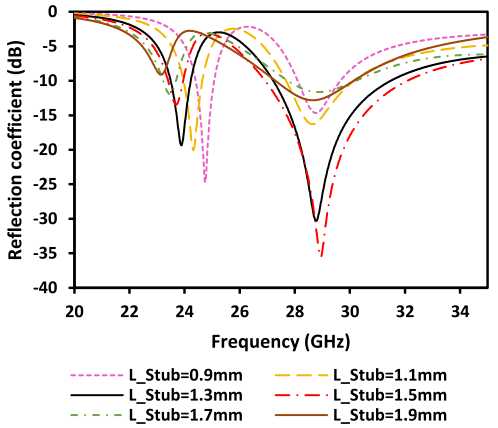

FIGURE 7. Effect of changing the open-circuited series stub.

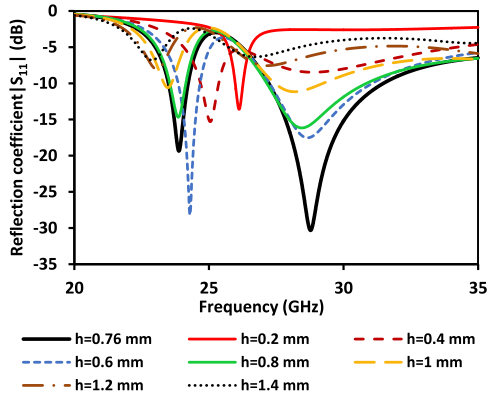

FIGURE 8. Effect of changing the substrate thickness on $|S_{11}|$.

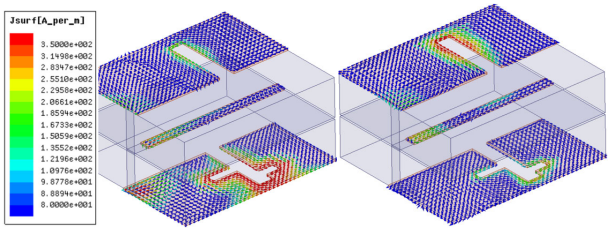

FIGURE 9. Surface current distribution at (a) f_1 and (b) f_2.

thickness (h) is changed by step 0.2 *mm* on a range from 0.2 to 1.4 *mm*. As cleared form the figure, good matching at the two frequencies (f_1 and f_2) is between $h = 0.6$ *mm* and $h = 0.8$ *mm*. Hence, $h = 0.75$ *mm* is chosen as the best point between them, for commercial material availability, the antenna is designed on standard Rogers Duroid substrate with a thickness of $h = 0.76$ *mm*. Moreover, the surface current distribution of the proposed antenna at the two frequencies is illustrated in Fig. 9 that clarify the field distribution for each resonator at f_1 and f_2.

B. ANTENNA RADIATION CHARACTERISTICS

The 2D normalized co-polarization and cross polarization of the radiation patterns in E-plane and H-plane at f_1 and f_2 are illustrated in Fig. 10 and Fig. 11, respectively. 3D of

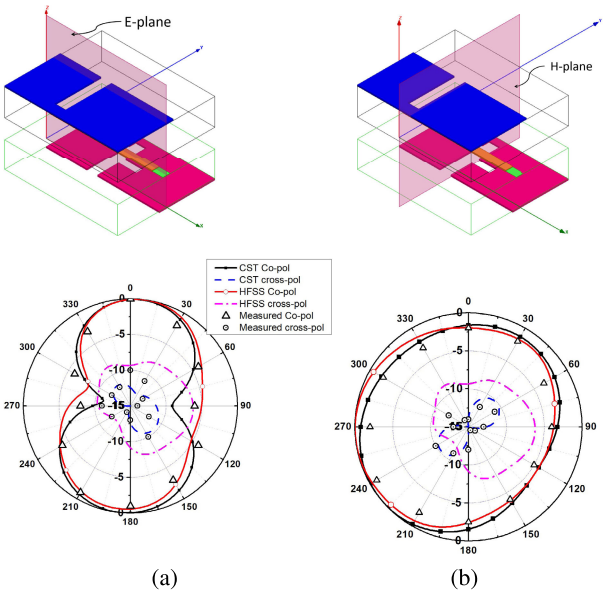

FIGURE 10. Simulated 2D radiation patterns of E-plane and H-plane at f_1 (a) E-plane and (b) H-plane.

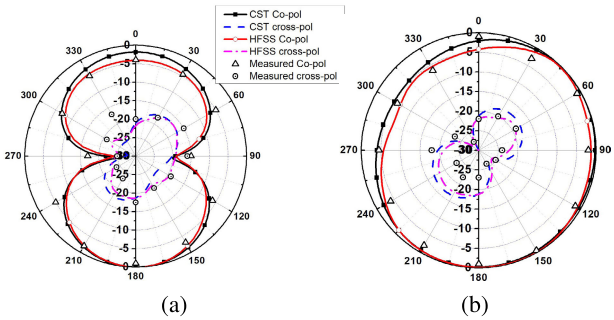

FIGURE 11. Simulated 2D radiation patterns of E-plane and H-plane at f_2 (a) E-plane and (b) H-plane.

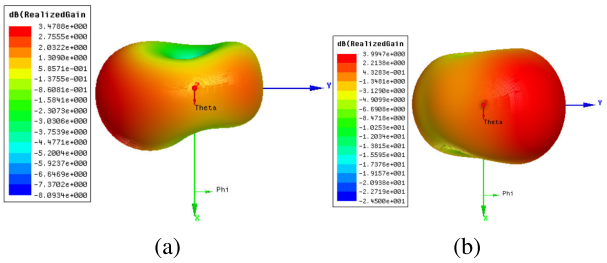

FIGURE 12. 3D radiation pattern at (a) f_1 and (b) f_2.

the antenna radiation patterns at two operating frequencies (f_1 and f_2) is revealed in Fig. 12 in order to show the directional characteristics (end-fire) of the proposed Open-ended quarter-wave half-slot resonator.

Due to the limitations in our experiments of the radiation characteristics at this high frequency band, the antenna's radiation patterns was measured using the system shown in Fig. 13. Anritsu 37269D Vector Network Analyzer was used in the measurements. The radiation pattern is measured manually by measuring the $|S_{21}|$ at every 30° degrees rotation for the proposed antenna in the Azimuth plane. A reference

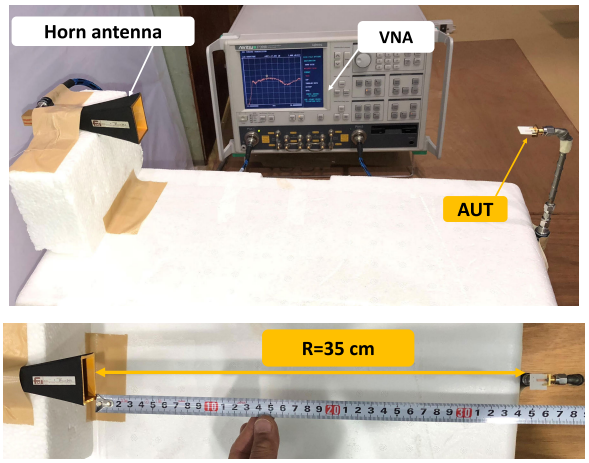

FIGURE 13. Radiation pattern measurement setup.

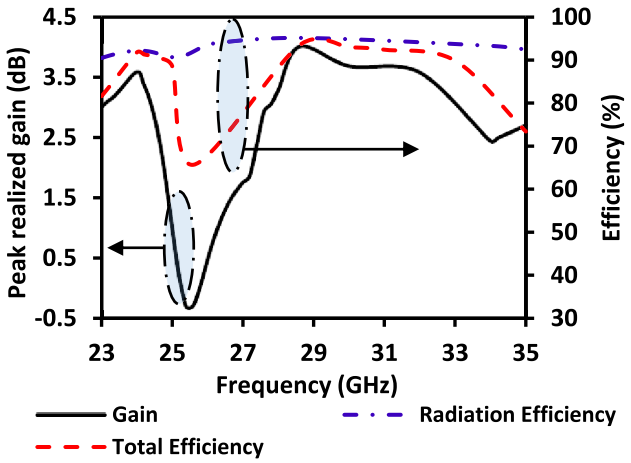

FIGURE 14. Peak realized gain as well as radiation and total efficiency versus frequency.

horn antenna (FMI 22240-20) is used as transmitter, while the proposed antenna is used as a receiver. Due to the low accuracy of the manual measurements, the radiation patterns are also verified with CST Microwave Studio simulator. Figs. 10 and 11 show that there is a good agreement between the two EM simulators results. The measured antenna gain has been calculated using Friis transmission equation:

$$|S_{21}| = \frac{P_r}{P_t} = G_t G_r (\frac{\lambda}{4\pi r})^2 \quad (1)$$

where P_r is the received power, P_t is the transmitted power, G_t is the gain of the transmitting antenna, G_r is the gain of the receiving antenna, r is the distance between the receiving and transmitting antennas, λ is the free-space wavelength and $|S_{21}|$ is the measured transmission coefficient between the two ports of the VNA (port 1 and Port 2).

The measured antenna gains at the two frequencies are 3.5 *dBi* and 4 *dBi* at f_1 and f_2, respectively. Also, the simulated radiation efficiencies are 92% and 95% at the same frequencies. Fig. 14 illustrates the values of peak realized gain, in dB, in addition to the values of the antenna radiation

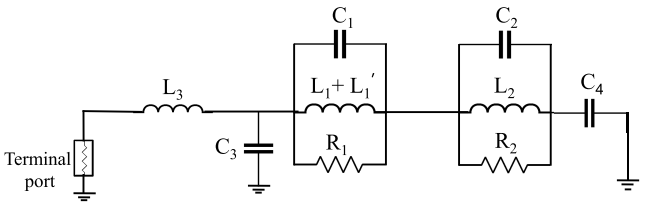

FIGURE 15. Antenna equivalent circuit, where the optimized circuit values are $C_1 = 1.97\ pF$, $L_1 + L_1' = 23\ pH$, $R_1 = 56.5\Omega$, $C_2 = 0.714\ pF$, $L_2 = 42\ pH$, $R_2 = 55.4\Omega$, $L_3 = 18\ pH$, $C_3 = 0.1\ fF$ and $C_4 = 3.6\ pF$.

TABLE 1. Elements values of equivalent circuit.

Frequency band	C_p	L_p
$f_{c1} = 23.5GHz$ $f_{01} = 23.88$GHz	$C_1 = 2.08pF$	$L_1 = 21.35pH$
$f_{c2} = 27.2GHz$ $f_{02} = 28.5GHz$	$C_2 = 0.6pF$	$L_2 = 52.2pH$

efficiency and total efficiency versus a range of frequency from 23 to 35 *GHz*. Total efficiency is the radiation efficiency multiplied by the mismatch efficiency that is represented in the reflection coefficient. Therefore, the values of the total efficiency is close to that of the radiation efficiency at the operating frequencies. On the other hand, due to the mismatching at other frequencies, it has low values of efficiency.

IV. EQUIVALENT CIRCUIT OF THE PROPOSED ANTENNA

The most challenge of designing the equivalent circuit is how to find an accurate model of the proposed antenna at the two resonance frequencies. Fig. 15 shows the equivalent circuit that used to model the electrical attitude of the proposed antenna. R, L, and C are used to implement the equivalent circuit model. As shown in Fig. 15, each QWHSR can be represented by a parallel RLC resonator; the resonance frequency of each one can be determined from equation (2). Firstly, each resonator is studied separately. S-parameters are calculated from Agilent ADS simulator for each resonator separetely, then the two resonators are combined in series. The initial values of L and C for each resonator can be calculated from equations (3) and (4) [20]. Where, C_p is the capacitance in picofarad and L_p is the inductance in nanohenry. The resonant and cutoff frequencies (f_0 and f_c in gigahertz, respectively) are determined from the HFSS simulator. Table 1 summarizes the initial values of C and L at the two operating frequencies.

$$f_r = \frac{1}{2\Pi\sqrt{LC}} \quad (2)$$

$$C_p = \frac{5f_c}{\Pi[f_0^2 - f_c^2]} pF \quad (3)$$

$$L_p = \frac{250}{c_p[\Pi f_0]^2} nH \quad (4)$$

TABLE 2. Comparison with some published work.

Ref.	Antenna type	Operating frequency (Bandwidth)	Gain (dBi)	Size $\lambda_g \times \lambda_g$ (mm^2)
[8]	Broadband dipole antenna	$32(26.5-38.2)GHz$	5	0.71×1.58
[9]	Wideband array (4 elements)	$27.5(23-32)GHz$	10-12	0.73×2.91
[10]	Slot antenna prototype I (broadband) prototype II (dualband)	31.5(20-40)GHz $28/38GHz$	5.3 & 5.36	0.78×0.78 & 0.7×0.7
[11]	Vertically stacked folded dipole	28 (27.5-29.5) GHz	5.67	0.84×0.84
[13]	Vivaldi antenna array (8 elements)	26(24.6-28.5)GHz	11.2	2.99×6.22
[14]	Tilted combined beam antenna	28 (27.5-28.5) GHz	7.3	2.76×4.15
This work	Dual-band half slot antenna	24 (23.47-25) GHz & 28.5 (27.2-31.7) GHz	3.5 & 4	0.37×0.44 & 0.44×0.52

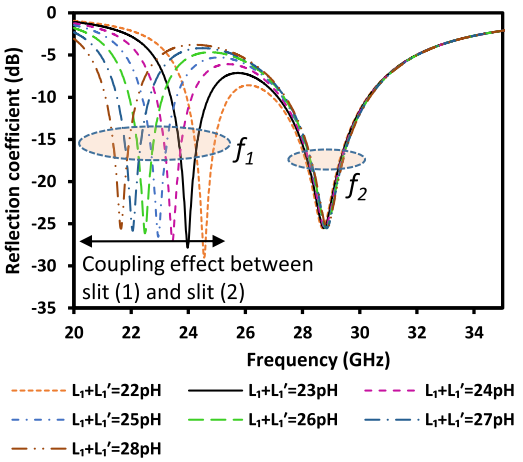

FIGURE 16. Effect of the coupling between slit (1) and slit (2).

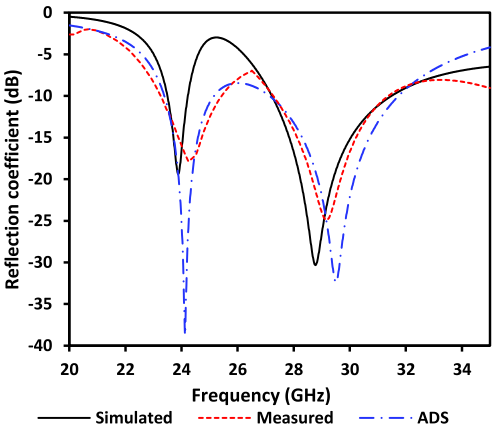

FIGURE 17. Simulated, measured and ADS results of $|S_{11}|$.

The loss resistance can be determined from the quality factor (Q)-frequency bandwidth relationship (BW) as:

$$Q = \frac{\omega_0}{BW} = \omega_0 RC \tag{5}$$

Where, the half power frequency bandwidth is evaluated from:

$$BW = \frac{1}{RC} \tag{6}$$

Then, the loss resistance (R) for each resonator can be determined from equation (7)

$$R = \frac{1}{BW \times C} \tag{7}$$

After combining the two resonators, taking into account the effect of losses resistances (R_1 and R_2) and the discontinuities at the two half slots edges (represented in a parallel capacitor (C_3)) in addition to making optimization, the final equivalent circuit can be obtained. The effect of the changing in the inductive coupling between slit (1) and slit (2) is studied in ADS simulator as shown in Fig. 16, where L_1' part refers to the value of the inductance due to the coupling between the slits. The simulated results of HFSS and ADS antenna equivalent circuit in addition to the measured results of the antenna reflection coefficient at the two resonant frequencies are shown in Fig. 17. Table 2 gives a comparison of the proposed antenna with published mm-waves antennas.

V. 2 x 2 MIMO SYSTEM FOR THE PROPOSED QWHS ANTENNA

MIMO antenna arrays are used for multiplexing and diversity in order to improve the signal-to-interference ratio and achieve high reliability of the communication system. Four elements MIMO array is tested using the proposed antenna element to get a good results and high isolation. A structure of 2 × 2 MIMO system, which is illustrated in Fig. 18, displays the position and the feeding of four QWHSR antennas. K connector model, which support the operation up to 40 GHz, is used in the simulation to get more accurate results. Fig. 19 shows the effect of the coupling between Ant. 1 and other three antennas (Ant.2, Ant.3 and Ant.4), Ant.2 has the largest coupling effect because it is the nearest antenna.

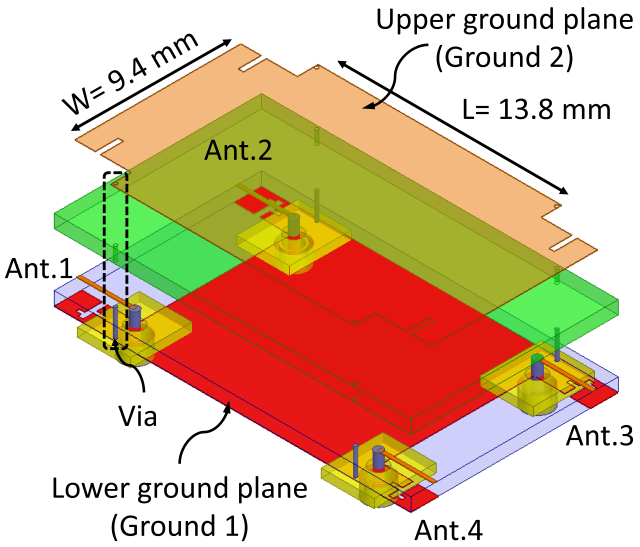

FIGURE 18. 2 × 2 MIMO system for the QWHS antenna.

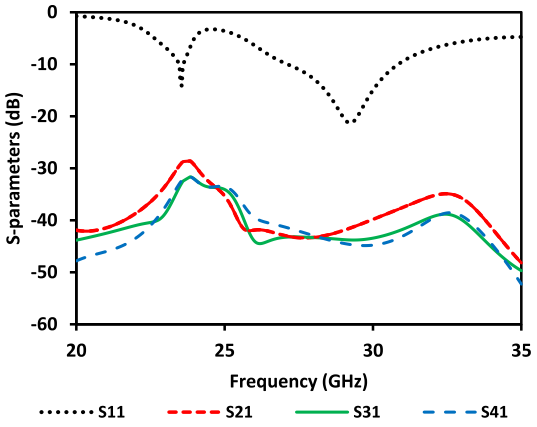

FIGURE 19. S-parameters for the proposed MIMO system.

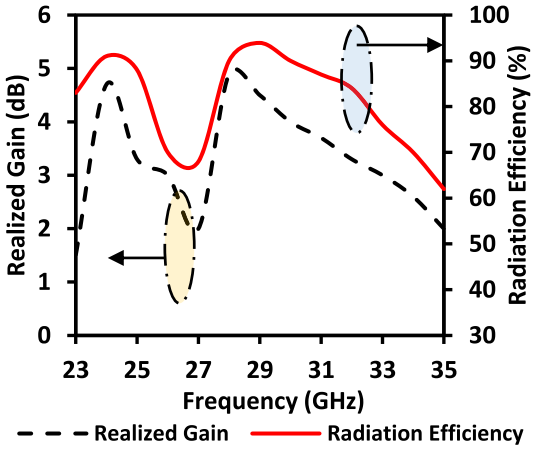

FIGURE 20. Radiation characteristics of the MIMO system.

However, in general the coupling characteristics are acceptable for MIMO system operation. The simulated results of radiation characteristics also are displayed in Fig. 20, antenna realized gain is slightly improved due to the large area of the ground plane to reach 4.7 *dB* and 4.9 *dB* at 24 *GHz* and 28 *GHz*, respectively.

VI. CONCLUSION

A new compact dual-band quarter-wave half-slot antenna for quasi-millimeter wave applications is discussed in this paper; The antenna works at 24 *GHz* and 28.5 *GHz* frequency bands with gains and radiation efficiencies of 3.5 *dBi*, 92%, 4 *dBi*, and 95% at f_1 and f_2, respectively. Antenna equivalent circuit is introduced to show the electrical behavior of the proposed design for active devices integration purposes. The proposed antenna is a good candidate for 5G wireless communication applications. The proposed antenna is employed in MIMO array composed of four elements. MIMO systems gives good results for the s-parameters as well as the radiation characteristics.

REFERENCES

[1] Y. Niu, Y. Li, D. Jin, L. Su, and A. V. Vasilakos, "A survey of millimeter wave communications (mmWave) for 5G: Opportunities and challenges," *Wireless Netw.*, vol. 21, no. 8, pp. 2657–2676, Nov. 2015. doi: 10.1007/s11276-015-0942-z.

[2] W. Roh, J. Y. Seol, J. Park, B. Lee, J. Lee, Y. Kim, J. Cho, K. Cheun, and F. Aryanfar, "Millimeter-wave beamforming as an enabling technology for 5G cellular communications: Theoretical feasibility and prototype results," *IEEE Commun. Mag.*, vol. 52, no. 2, pp. 106–113, Feb. 2014.

[3] X.-F. Zhang, J.-X. Fan, and J.-X. Chen, "High gain and high-efficiency millimeter-wave antenna based on spoof surface plasmon polaritons," *IEEE Trans. Antennas Propag.*, vol. 67, no. 1, pp. 687–691, Jan. 2019.

[4] W. Hong, K.-H. Baek, Y. Lee, Y. Kim, and S.-T. Ko, "Study and prototyping of practically large-scale mmWave antenna systems for 5G cellular devices," *IEEE Commun. Mag.*, vol. 52, no. 9, pp. 63–69, Sep. 2014.

[5] A. I. Sulyman, A. T. Nassar, M. K. Samimi, G. R. MacCartney, Jr., T. S. Rappaport, and A. Alsanie, "Radio propagation path loss models for 5G cellular networks in the 28 GHz and 38 GHz millimeter-wave bands," *IEEE Commun. Mag.*, vol. 52, no. 9, pp. 78–86, Sep. 2014.

[6] G. R. Maccartney, T. S. Rappaport, S. Sun, and S. Deng, "Indoor office wideband millimeter-wave propagation measurements and channel models at 28 and 73 GHz for ultra-dense 5G wireless networks," *IEEE Access*, vol. 3, pp. 2388–2424, 2015.

[7] X. Li, J. Xiao, Z. Qi, and H. Zhu, "Broadband and high-gain SIW-fed antenna array for 5G applications," *IEEE Access*, vol. 6, pp. 56282–56289, 2018.

[8] S. X. Ta, H. Choo, and I. Park, "Broadband printed-dipole antenna and its arrays for 5G applications," *IEEE Antennas Wireless Propag. Lett.*, vol. 16, pp. 2183–2186, 2017.

[9] S. Ershadi, A. Keshtkar, A. H. Abdelrahman, and H. Xin, "Wideband high gain antenna subarray for 5G applications," *Prog. Electromagn. Res.*, vol. 78, pp. 33–46, 2017.

[10] N. Ashraf, O. M. Haraz, M. M. M. Ali, M. A. Ashraf, and S. A. S. Alshebili, "Optimized broadband and dual-band printed slot antennas for future millimeter wave mobile communication," *AEU-Int. J. Electron. Commun.*, vol. 70, no. 3, pp. 257–264, 2016.

[11] I.-J. Hwang, H.-W. Jo, J.-W. Kim, G. Kim, J.-W. Yu, and W.-W. Lee, "Vertically stacked folded dipole antenna using multi-layer for mm-Wave mobile terminals," in *Proc. IEEE Int. Symp. Antennas Propag. USNC/URSI Nat. Radio Sci. Meeting*, Jul. 2017, pp. 2579–2580.

[12] M. H. Dahri, M. Inam, M. H. Jamaluddin, and M. R. Kamarudin, "A review of high gain and high efficiency reflectarrays for 5G communications," *IEEE Access*, vol. 6, pp. 5973–5985, 2017.

[13] S. Zhu, H. Liu, Z. Chen, and P. Wen, "A compact gain-enhanced Vivaldi antenna array with suppressed mutual coupling for 5G mmWave application," *IEEE Antennas Wireless Propag. Lett.*, vol. 17, no. 5, pp. 776–779, May 2018.
[14] J. S. Park, J.-B. Ko, H.-K. Kwon, B.-S. Kang, B. Park, and D. Kim, "A tilted combined beam antenna for 5G communications using a 28-GHz band," *IEEE Antennas Wireless Propog. Lett*, vol. 15, pp. 1685–1688, 2016.
[15] N. Hussain, M. Jeong, J. Park, and N. Kim, "A broadband circularly polarized Fabry–Pérot resonant antenna using a single-layered PRS for 5G MIMO applications," *IEEE Access*, vol. 7, pp. 42897–42907, 2019.
[16] Y. M. Pan, X. Qin, Y. X. Sun, and S. Y. Zheng, "A simple decoupling method for 5G millimeter-wave MIMO dielectric resonator antennas," *IEEE Trans. Antennas Propag.*, vol. 67, no. 4, pp. 2224–2234, Apr. 2019.
[17] Y. Zhang, J.-Y. Deng, M.-J. Li, D. Sun, and L.-X. Guo, "A MIMO dielectric resonator antenna with improved isolation for 5G mm-Wave applications," *IEEE Antennas Wireless Propag. Lett.*, vol. 18, no. 4, pp. 747–751, Apr. 2019.
[18] S.-J. Park, M.-H. Jeong, K.-B. Bae, D.-C. Kim, L. Minz, and S.-O. Park, "Performance comparison of 2 × 2 MIMO antenna arrays with different configurations and polarizations in reverberation chamber at millimeter-waveband," *IEEE Trans. Antennas Propag.*, vol. 65, no. 12, pp. 6669–6678, Dec. 2017.
[19] M. Aboualalaa, A. B. Abdel-Rahman, A. Allam, H. Elsadek, K. Yoshitomi, and R. K. Pokharel, "Compact 24 GHz half-slot antenna for energy combining," in *Proc. Int. Appl. Comput. Electromagn. Soc. Symp. (ACES)*, Mar. 2018, pp. 1–2.
[20] A. B. Abdel-Rahman, A. K. Verma, A. Boutejdar, and A. S. Omar, "Control of bandstop response of Hi-Lo microstrip low-pass filter using slot in ground plane," *IEEE Trans. Microw. Theory Techn.*, vol. 52, no. 3, pp. 1008–1013, Mar. 2004.

MOHAMED ABOUALALAA received the B.S. degree in electronics and communications engineering from Menofia University, Egypt, in 2009, the M.S. degree in electronics and communications engineering from Cairo University, Egypt, in 2014, and the Ph.D. degrees in electronics and communications engineering from the Egypt-Japan University of Science and Technology (E-JUST), Alexandria, Egypt, in 2018.

He was a special research student with Kyushu University, Japan, from 2017 to 2018. From 2010 to 2013, he was a Research Assistant with the Microstrip Circuits Department, Electronics Research Institute, Egypt, where he was an Assistant Researcher, from 2014 to 2015. He is currently a Researcher with the Electronics Research Institute. His research interests include microwave planar antennas, reconfigurable antennas, energy harvesting, and wireless power transfer.

ISLAM MANSOUR received the B.Sc. degree in electrical and electronic engineering from Benha University, Cairo, Egypt, in 2010, and the M.Sc. degree in electrical and electronic engineering from Ain Shams University, Cairo, Egypt, in 2015, and the Ph.D. degree in electronics and communications engineering from the Egypt-Japan University of Science and Technology (E-JUST), Alexandria, Egypt, in 2019. She was a special research student with Kyushu University, from 2017 to 2018, Japan. She is currently the Doctor with the Department of Electrical and Electronic Engineering, Shoubra Faculty of Engineering, Benha University, Egypt. She is also involved in millimeter-wave frequency generation circuit design and its applications.

HALA ELSADEK graduated from Ain Shams University, Cairo, Egypt, in 1991. She received the master's degree, Japan, in 1996, and the Ph.D. degree from the University of California, Irvine, CA, USA, in 2002. She is currently a Professor and the Microstrip Department Head, as well as the Technology Development Committee Director of the Electronics Research Institute. Her research interests include RF wireless communications, electromagnetic engineering, and microstrip antenna systems. She acts in editorial boards in several journals. She has five books and holds six patents. She is also a single and coauthor in more than 150 articles. She is also a supervisor on master's and Ph.D. theses in different universities in Egypt and abroad, such as Japan and USA. She participates in more than 35 research and development projects at the national and international levels. Her role is from PI to C-PI. She was a recipient of several prizes as Women in Innovation Certificate from the Academy of Scientific Research and Technology, Egypt, 2018, the Silver Medal from Kuwait 10th international invention Fair in the middle East, 2018, Cambridge International College, Certificate of Recognition, December 2107, the Award of Recognition in the Fourth Cairo Innovates Exhibition 2017 for the role in the National Alliance for Deepen local manufacturing in Electronics Industry in Egypt and the Award for the First Best Researcher in Electronics Research Institutes, in 2019. She is included in several biographical indexes and acts as reviewer in many international societies in her field as the IEEE AP-S and MTT.

ADEL B. ABDEL-RAHMAN was born in Aswan, Egypt. He received the B.S. and M.S. degrees in electrical engineering, communication, and electronics from Assiut University, Egypt, and the Dr.-Ing. degree in communication engineering from Otto von Guericke University, Germany, in 2005. Since October 2006, he has been an Assistant Professor with the Electrical Engineering Department, South Valley University, Qena, Egypt, where he was the Executive Director of information and communication technology, from 2010 to 2012. Since October 2012, he has been with the School of Electronics, Communications and Computer Engineering, Egypt-Japan University of Science and Technology (E-JUST), Alexandria, Egypt. He was the Dean of the Faculty of Computers and Information, South Valley University, from 2016 to 2018. He is currently a Professor with the Department of Electronics and Communications Engineering, Egypt-Japan University of Science and Technology. He has published more than 120 refereed journal and conference articles. He has two patents. He also holds one patent (DE10322803A1) and one book (ISBN: 978-981-13-8047-1). His research interests include the design and analysis of antennas, filters, millimeter-wave devices, WPT, and metamaterials and their application in wireless communication, as well as optimization techniques with applications to microwave devices and antenna arrays.

AHMED ALLAM received the B.Sc. degree in electrical engineering from Alexandria University, Alexandria, Egypt, and the M.Eng. and Ph.D. degrees from the University of Alberta, Edmonton, AB, Canada. From April 1994 to January 1998, he was an Instrument Engineer with Schlumberger. From May 2000 to September 2001, he was with Murandi Communications Ltd., Calgary, AB, Canada, where he worked on RF transceivers design. From April 2007 to April 2008, he worked on RF CMOS transceivers design with Scanimetrics Inc., Edmonton. He is currently an Associate Professor with the Department of Electronics and Communications Engineering, Egypt-Japan University of Science and Technology, Alexandria, Egypt. His research interest includes the design of RF circuits and systems.

MOHAMMED ABO-ZAHHAD received the B.S.E.E. and M.S.E.E degrees in electrical engineering from Assiut University (AU), Egypt, in 1979 and 1983, respectively, and the Ph.D. degree from the University of Kent, Canterbury, U.K., and AU (channel system), in 1988.

He promoted to an Associate Professor and a Professor of electronics and communication engineering, in December 1993 and January 1999, respectively. He has also been a Professor of electronics and communication engineering, since January1999, the Dean of the School of Electronics, Communication and Computer Engineering, a Professor of communication and electronics engineering with the Egypt-Japan University of Science and Technology (E-JUST), since January 2017. He was elected as the Vice-Dean for graduated studies, from August 2006 to June 2012, and the Chair of the Electrical and Electronics Department, from November 2013 to December 2016, both in the Faculty of Engineering, AU. In April 2018, he was selected by the ministry of higher education as an expert for setting the study plans and regulations for new constructed universities in Egypt. He is currently the General Director of the E-JUST Information and Communication Technology Center. His research interests include switched-capacitor, optical and digital filters, biomedical and genomic signal processing, speech processing, data compression, wavelet-transforms, genetic algorithms, immune algorithms, wireless sensor networks, and electronic systems. He has published more than 160 articles in national and international journals and conferences in the above fields. He is a member of the European Society of Circuit Theory and Applications, in 1998. He has been a consultant of the Management Information Systems, Project Management Unit (PMU), Ministry of Higher Education, a member of the National Communication and Electronics Promotion Committee, as well as a Reviewer of the National Quality Assurance and Accreditation Authority, NAQQA, Egypt, since 2011.

KUNIAKI YOSHITOMI (M'93) received the B.S. and M.S. degrees in electronics and D.E. degree in communication engineering from Kyushu University, Fukuoka, Japan, in 1979, 1981, and 1986, respectively, where he joined the Faculty of Engineering, in 1981. From 1990 to 1991, he was with the Department of Electrical Engineering, University of Washington, Seattle, WA, USA, as a Visiting Associate Professor. He is currently a Professor with the Center for Japan–Egypt Cooperation in Science and Technology, Kyushu University. His current research interests include antennas, scattering and diffraction, inverse problem, and electromagnetic compatibility.

RAMESH K. POKHAREL (M'04) received the M.E. and Ph.D. degrees in electrical engineering from the University of Tokyo, Japan, in 2000 and 2003, respectively. He was a Postdoctoral Research Fellow with the Department of Electrical Engineering and Electronics, Aoyama Gakuin University, Japan, from April 2003 to March 2005. In April 2005, he joined the Department of Electronics, Graduate School of Information Science and Electrical Engineering, Kyushu University, where he has been a Professor, since October 2010. His current research interests include the low-cost RFIC and analog circuits for microwave and millimeter wave wireless communications, on-chip signal integrity issues, on-chip meta-materials in CMOS, and near-field wireless power transfer system through human tissues. He was a recipient of the Monbu-Kagakusho (MEXT) Scholarship of the Japanese Government, from 1997 to 2003, an excellent Center of Excellence (COE) Research Award from the University of Tokyo, in 2003, and the Best ELEX Paper Award in 2017 by the IEICE, Japan. He served as the Deputy-Director for the Center for Egypt-Japan Cooperation in Science and Technology, Kyushu University, from April 2012 to March 2014, where served as the Director, from April 2014 to March 2017. He also served as a Secretary of the IEEE MTT-S Japan Society, from January 2012 to December 2013, and as the Vice-Chair of the Education committee of the IEEE-MTT-S Japan Society, from January 2014 to December 2016, where he has been serving as the Chair, since January 2017.